

Synthesis and Characterization of Polynuclear Copper(II) Complexes with Pyridylbis(phenol) Ligands

Rajendra Shakya, Anna Jozwiuk, Douglas R. Powell, and Robert P. Houser*

Department of Chemistry and Biochemistry, University of Oklahoma, Norman, Oklahoma, 73019

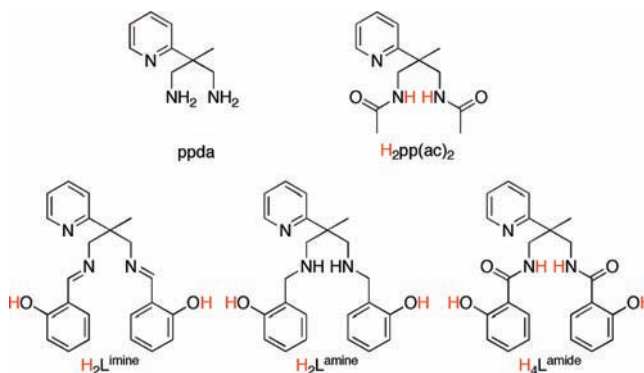
Received November 13, 2008

Three new pyridylbis(phenol) ligands with imine (H_2L^{imine}), amine (H_2L^{amine}), or amide (H_4L^{amide}) linkages, along with their copper complexes, were synthesized and characterized. Treatment of H_2L^{imine} with copper(II) in the presence of base produced mononuclear copper complex $[Cu(L^{\text{imine}})(MeOH)]$ (**1**), while the same procedure with H_2L^{amine} produced trinuclear $[Cu_3(L^{\text{amine}})_2(CH_3CN)_2](ClO_4)_2$ (**2**). The more rigid H_4L^{amide} forms tetranuclear $[Cu_4(L^{\text{amide}})_2(H_2O)_4]$ (**3**), which upon recrystallization yielded crystals of hexanuclear $[Cu_6(HL^{\text{amide}})_4(H_2O)_2]$ (**4**).

Introduction

The design and synthesis of new ligands that support polynuclear transition metal complexes and/or clusters are often inspired by systems in bioinorganic, materials, and catalysis chemistry. Our laboratory has generated a family of pyridyl amide ligands that were used to synthesize a number of transition metal species of various nuclearity and oxidation states.^{1–3} More recently, we extended our family of ligands to include pyridylbis(phenol) $H_2pp(ac)_2$ (Scheme 1), which was found to support a novel trinuclear mixed-valence complex.³ Here we report three new ligands that share a common backbone with $H_2pp(ac)_2$. The new ligands contain phenol groups in place of the methyl groups on $H_2pp(ac)_2$. Copper complexes with phenol-containing ligands have received considerable attention because of their relevance to the fungal enzyme galactose oxidase,⁴ with recent progress in biomimetic model complexes summarized in several excellent reviews.⁵ Indeed, our new ligands bear a strong resemblance to a class of tetradentate salen ligands

Scheme 1. Ligands Used in This Study (Bottom), Precursor $ppda$ (Top), and Related $H_2pp(ac)_2$ (Top)^a



^a Ionizable protons are highlighted in red.

possessing an N_2O_2 donor set,^{6,7} but with the addition of a pyridyl N-donor. While one ligand (H_4L^{amide}) shares the same amide groups as $H_2pp(ac)_2$, the other two contain imine (H_2L^{imine}) and amine (H_2L^{amine}) linkages.

Experimental Section

General Procedures. Unless otherwise stated, all reagents were used as received from commercial sources. The starting material for all three ligands, 2-methyl-2-pyridin-2-yl-propane-1,3-diamine

* To whom correspondence should be addressed. E-mail: houser@ou.edu.

- (1) (a) Klein, E. L.; Khan, M. A.; Houser, R. P. *Inorg. Chem.* **2004**, *43*, 7272–7274. (b) Mondal, A.; Li, Y.; Khan, M. A.; Ross, J. H.; Houser, R. P. *Inorg. Chem.* **2004**, *43*, 7075–7082. (c) Pal Chaudhuri, U.; Whiteaker, L. R.; Yang, L.; Houser, R. P. *Dalton Trans.* **2006**, 1902–1908. (d) Yang, L.; Houser, R. P. *Inorg. Chem.* **2006**, *45*, 9416–9422. (e) Pal Chaudhuri, U.; Whiteaker, L. R.; Mondal, A.; Klein, E. L.; Powell, D. R.; Houser, R. P. *Inorg. Chim. Acta* **2007**, *360*, 3610–3618.
- (2) Yang, L.; Powell, D. R.; Houser, R. P. *Dalton Trans.* **2007**, 955–964.
- (3) Yang, L.; Powell, D. R.; Klein, E. L.; Grohmann, A.; Houser, R. P. *Inorg. Chem.* **2007**, *46*, 6831–6833.
- (4) Whittaker, J. W. *Chem. Rev.* **2003**, *103*, 2347–2363.
- (5) (a) Itoh, S.; Taki, M.; Fukuzumi, S. *Coord. Chem. Rev.* **2000**, *198*, 3–20. (b) Jazdzewski, B. A.; Tolman, W. B. *Coord. Chem. Rev.* **2000**, *200*, 633–685. (c) Thomas, F. *Eur. J. Inorg. Chem.* **2007**, 2379–2404.

- (6) Kitajima, N.; Whang, K.; Morooka, Y.; Uchida, A.; Sasada, Y. *J. Chem. Soc., Chem. Commun.* **1986**, 1504–1505.
- (7) (a) Chaudhuri, P.; Hess, M.; Müller, J.; Hildenbrand, K.; Bill, E.; Weyhermüller, T.; Wieghardt, K. *J. Am. Chem. Soc.* **1999**, *121*, 9599–9610. (b) Pratt, R. C.; Stack, T. D. P. *Inorg. Chem.* **2005**, *44*, 2367–2375. (c) Pratt, R. C.; Stack, T. D. P. *J. Am. Chem. Soc.* **2003**, *125*, 8716–8717.

(ppda), was synthesized according to the literature procedure.⁸ The solvents used were doubly purified using alumina columns in a MBraun solvent purification system (MB-SPS). Infrared spectra were measured from 4000 to 400 cm^{-1} as KBr pellets on a NEXUS 470 FTIR spectrometer. ^1H NMR spectra were measured using a Varian 300 MHz instrument. Electrospray Ionization (ESI; positive) spectra were measured in a quadrupole time-of-flight mass spectrometer (Q-TOF; Micromass, Manchester, U.K.) containing a Z-spray ESI source. Elemental analyses were performed by Atlantic Microlab, Norcross, GA. UV/vis spectra of dichloromethane solutions of **1** and **2** and DMSO solutions of **3** were measured using a Shimadzu UV2401PC spectrophotometer in the range 250 to 1100 nm on solutions of variable concentration (8×10^{-6} – 1×10^{-3} M). Cyclic voltammetry experiments were performed using a BAS 50W potentiometer. A standard three-electrode-cell was employed with a glassy-carbon working electrode, a Pt-wire auxiliary electrode, and an Ag/AgCl reference electrode under an inert atmosphere at room temperature. X-Band EPR spectra of the complexes were recorded using Bruker EMX spectrometer in dichloromethane for **1** and **2** and DMSO for **3** at 77 K in frozen solutions. The EPR parameters were obtained from spectral simulations using the programs Simfonia (Version 1.25, Bruker Instruments Inc.) and Bruker WINEPR-System (Version 2.11, Bruker-Franzen Analytik GmbH). Solution magnetic moment measurements were measured using the Evans method.⁹ Solid state magnetic susceptibility was measured using a Johnson Matthey/Fabricated Equipment Magnetic Susceptibility Balance (MSB-AUTO) with magnetic field strength 4.5 kG, and a measurement range of $\pm 1.999 \times 10^{-4}$ to $\pm 5 \times 10^{-10}$ cgs. The MSB-AUTO possesses a detector that is based on the Evan's design and measures the susceptibility by detecting the force acting upon a suspended magnet. A narrow bore sample tube with 0.400 cm outer diameter and 0.200 cm inner diameter was used. Dry powdered samples were packed by tapping the tube up to the minimum height of 15 mm. The TARE function was used to operate at gain E-6. Mass susceptibility was recorded following the input of the sample length and the sample weight.

Caution! Perchlorate salts of metal complexes with the organic ligands are potentially explosive. Although no difficulty was encountered during the synthesis, they should be prepared in small amounts and handled with caution.

2,2'-(2-Methyl-2-(pyridin-2-yl)propane-1,3-diyl)bis(azan-1-yl-1-ylidene)bis(methan-1-yl-1-ylidene)diphenol ($\text{H}_2\text{L}^{\text{imine}}$). The ligand $\text{H}_2\text{L}^{\text{imine}}$ was prepared by the Schiff base condensation of ppda (0.820 g, 5.00 mmol) with salicylaldehyde (1.22 g, 10.0 mmol) in a 50 mL MeOH solution. The solution was stirred at 50 °C for 2 h, yielding a pale yellow solution which was then allowed to cool to room temperature. The yellow precipitate formed was filtered and then washed with cold methanol. The product was dried under vacuum for several hours (1.54 g, 83% yield). Anal. Calcd for $\text{C}_{23}\text{H}_{23}\text{N}_3\text{O}_2$: C, 74.0; H, 6.2; N 11.2. Found: C, 74.0; H, 6.2; N, 11.3. ^1H NMR (300 MHz, CDCl_3 , 293 K) δ 1.54 (s, 3H), 4.00 (d, $J = 12.3$ Hz, 2H), 4.14 (d, $J = 12.3$ Hz, 2H), 6.84–7.30 (m, 8H), 7.20–7.70 (m, 3H), 8.33 (s, 2H), 8.57 (d, $J = 0.9$ Hz, 1H) ppm. FTIR (KBr): 3305 (O–H), 2999 (s, C–H), 2965 (s, C–H), 2862 (s, C–H), 1630 (s, C=N_{imine}), 1577 (s), 1498 (s, C=N_{py}, C=C_{aromatic}), 1474, 1458, 1422, 1378, 1334, 1278, 1210, 1118, 1038, 1019, 989, 949, 891, 857, 764, 655, 630, 587, 552, 476 cm^{-1} . ESI-MS pos. in MeOH: $m/z = 374$ [$\text{H}_2\text{L}^{\text{imine}} + \text{H}$]⁺.

2,2'-(2-Methyl-2-(pyridin-2-yl)propane-1,3-diyl)bis(azanediy)-bis(methylene)diphenol ($\text{H}_2\text{L}^{\text{amine}}$). The ligand $\text{H}_2\text{L}^{\text{amine}}$ was prepared by the condensation of ppda (0.820 g, 5.00 mmol) with the salicylaldehyde (1.22 g, 10.0 mmol) in a 50 mL MeOH solution. The solution was stirred at 50 °C for 2 h, yielding a pale yellow solution. NaBH_4 (0.570 g, 15.0 mmol) was then added at 0 °C in small portions. The solution was stirred at room temperature for 2 h, the solvent was evaporated, and the product amine was extracted with dichloromethane, dried over MgSO_4 and isolated after solvent evaporation (1.49 g, 79% yield). Anal. Calcd for $\text{C}_{23}\text{H}_{27}\text{N}_3\text{O}_2$: C, 73.2; H, 7.2; N, 11.1. Found: C, 73.0; H, 7.3; N, 11.0. ^1H NMR (300 MHz, CDCl_3 , 300 K) δ 1.50 (s, 3H), 2.92 (d, $J = 11.7$ Hz, 2H), 3.14 (d, $J = 11.7$ Hz, 2H), 3.94 (m, 4H), 6.80–7.30 (m, 8H), 7.20–7.80 (m, 3H), 8.57 (d, $J = 0.9$ Hz, 1H) ppm. FTIR (KBr): 3305 (O–H), 3006 (s, C–H), 2845 (s, C–H), 1613, 1586 (s), 1567, 1475 (s, C=N_{py}, C=C_{aromatic}), 1458, 1428, 1366, 1336, 1253, 1148, 1085, 1036, 979, 949, 913, 756, 720, 620, 470 cm^{-1} . ESI-MS pos. in MeOH: $m/z = 378$ [$\text{H}_2\text{L}^{\text{amine}} + \text{H}$]⁺.

N,N' -(2-methyl-2-(pyridin-2-yl)propane-1,3-diyl)bis(2-hydroxybenzamide) ($\text{H}_4\text{L}^{\text{amide}}$). The ligand $\text{H}_4\text{L}^{\text{amide}}$ was prepared by the coupling reaction of ppda with salicylic acid. To EDC·HCl (0.951 g, 4.96 mmol) dissolved in 10 mL of dichloromethane was added triethylamine (0.752 g, 7.44 mmol). Subsequently HOBt (0.670 g, 4.96 mmol) and salicylic acid (0.685 g, 4.96 mmol) were added to the previous mixture to obtain the active ester. In another flask ppda (0.410 g, 2.48 mmol) was dissolved in 10 mL of dichloromethane and cooled to 0 °C. The active ester was added dropwise to the solution of ppda. After the addition was completed the reaction mixture was allowed to warm to room temperature and stirred for 2 days. The solution was washed with water, dried over MgSO_4 and reduced in vacuum. The resulting thick yellow oil was purified by column chromatography (silica gel, hexane:ethyl acetate, 7: 3) to give $\text{H}_4\text{L}^{\text{amide}}$ as a white crystalline powder (0.620 g, 62% yield). Anal. Calcd for $\text{C}_{23}\text{H}_{23}\text{N}_3\text{O}_4$: C, 68.1; H, 5.7; N, 10.4. Found: C, 68.3; H, 5.8; N, 10.1. ^1H NMR (300 MHz, CDCl_3 , 293 K) δ 1.30 (s, 3H), 3.24 (d, $J = 12.0$ Hz, 2H), 4.25 (d, $J = 12.0$ Hz, 2H), 6.83–7.73 (m, 11H), 8.37 (d, $J = 0.9$ Hz, 1H), 8.55–8.56 (m, 1H), 12.39 (s, 1H) ppm. FTIR (KBr): 3347 (O–H), 3067 (s, C–H), 2972 (s, C–H), 2925 (s, C–H), 2776, 1726, 1637 (s, C=O_{amide}), 1596 (s), 1469 (s, C=N_{py}, C=C_{aromatic}) cm^{-1} . ESI-MS pos. in MeOH: $m/z = 406$ [$\text{H}_4\text{L}^{\text{amide}} + \text{H}$]⁺, and 428 [$\text{H}_4\text{L}^{\text{amide}} + \text{Na}$]⁺.

[Cu(L^{imine})(CH_3OH)] (1**).** To a 15 mL MeOH solution of $\text{H}_2\text{L}^{\text{imine}}$ (0.0930 g, 0.250 mmol) and Et_3N (0.10 mL: 0.70 mmol) was added dropwise a 1 mL MeOH solution of $\text{CuCl}_2 \cdot 2\text{H}_2\text{O}$ (0.070 g: 0.200 mmol). The resulting dark green solution was stirred for 2 h at room temperature and filtered to discard any unreacted solids. X-ray quality crystals were obtained from the solution after crystallization by slow evaporation of the solvent (0.0760 g, 70% yield). The sample for elemental analysis was powdered and dried under vacuum overnight, removing methanol solvent of crystallization from the complex. Anal. Calcd for $\text{C}_{23}\text{H}_{21}\text{CuN}_3\text{O}_2$: C, 63.5; H, 4.9; N 9.7. Found: C, 63.2; H, 4.8; N, 9.6. UV/vis (CH_2Cl_2) [λ_{max} , nm (ϵ , $\text{M}^{-1} \text{cm}^{-1}$): 373 (13,800), 608 (228). EPR (9.434 GHz, mod. amp. 20.0 G, CH_2Cl_2 , 77K): $g_{\parallel} = 2.21$, $g_{\perp} = 2.04$, and $A_{\parallel} = 190$ G. FTIR (KBr): 1622 (s, C=N_{imine}), 1569, 1535 (s), 1469 (s, C=N_{py}, C=C_{aromatic}), 1447, 1415, 1380, 1320, 1200, 1151, 1127, 1049, 901, 755, 740, 601, 571, 461 cm^{-1} . ESI-MS pos. in MeOH: $m/z = 435$ [$\text{Cu}(\text{L}^{\text{imine}}) + \text{H}$]⁺. Solution magnetic moment (Evans method, 19.8 °C, 17.0×10^{-3} M, acetonitrile- d_3): 1.805 μ_{B} /Cu. Solid state magnetic moment (MSB-Auto, 4.5 kG, 22.0 °C): 1.800 μ_{B} /Cu.

[Cu₃(L^{amine})₂(CH_3CN)₂](ClO_4)₂ (2**).** To a 5 mL acetonitrile solution of $\text{H}_2\text{L}^{\text{amine}}$ (0.0370 g, 0.100 mmol) and Et_3N (0.040 mL, 0.30 mmol) was added dropwise a 1 mL acetonitrile solution of

(8) Friedrich, S.; Schubart, M.; Gade, L. H.; Scowen, I. J.; Edwards, A. J.; McPartlin, M. *Chem. Ber./Recl.* **1997**, *130*, 1751–1759.

(9) Evans, D. F. *J. Chem. Soc.* **1959**, 2003–2005.

Table 1. Crystallographic Data for **1**, **2**, and **4**

	1 ·CH ₃ OH	2 ·C ₂ H ₃ N	4 ·4H ₂ O·2DMSO
formula	C ₂₅ H ₂₉ CuN ₃ O ₄	C ₅₂ H ₅₉ Cl ₂ Cu ₃ N ₉ O ₁₂	C ₉₈ H ₁₁₀ Cu ₆ N ₁₂ O ₂₅ S ₃
fw	499.05	1263.60	2333.40
crystal system	monoclinic	monoclinic	monoclinic
space group	<i>P</i> 2 ₁ / <i>c</i>	<i>P</i> 2 ₁ / <i>n</i>	<i>C</i> 2/ <i>c</i>
<i>a</i> (Å)	6.7197(8)	12.509(4)	25.131(6)
<i>b</i> (Å)	17.887(2)	12.155(4)	16.508(4)
<i>c</i> (Å)	19.157(2)	18.708(6)	27.977(7)
α (deg)	90	90	90
β (deg)	90.430(5)	99.208(8)	93.654(8)
γ (deg)	90	90	90
<i>V</i> (Å ³)	2302.5(4)	2807.8(16)	11583(5)
<i>Z</i>	4	2	4
ρ_{calcd} (mg/m ⁻³)	1.440	1.495	1.338
μ (mm ⁻¹)	0.986	1.289	1.206
θ (deg)	1.56 to 26.00	1.83 to 26.00	2.04 to 19.03
$R1,^a$ $wR2,^b$ $ I > 2\sigma(I)$	0.0289, 0.0784	0.0737, 0.2124	0.0828, 0.2625
GOF on F^2	1.006	1.026	1.076

$$^a R1 = \sum ||F_o| - |F_c|| / \sum |F_o|. \quad ^b wR2 = \{ \sum [w(F_o^2 - F_c^2)^2] / \sum w(F_o^2)^2 \}^{1/2}.$$

Cu(ClO₄)₂·6H₂O (0.0370 g, 0.100 mmol). The resulting dark green solution was stirred for 2 h at room temperature and filtered to remove any unreacted solids. X-ray quality crystals were obtained from the solution after crystallization by ether diffusion (0.034 g, 60% yield). The sample for elemental analysis was powdered and dried under vacuum overnight, removing acetonitrile solvent of crystallization from the complex. Anal. Calcd for C₄₆H₅₀Cl₂Cu₃N₆O₁₂: C, 48.4; H, 4.4; N 7.5. Found: C, 47.8; H, 4.6; N, 7.5. UV/vis (CH₂Cl₂) [λ_{max} , nm (ϵ , M⁻¹ cm⁻¹): 326 (2350), 398 (3130), 597 (343 sh)]. EPR (9.436 GHz, mod. amp. 5.0 G, CH₂Cl₂, 77K): $g_{\parallel} = 2.26$, $g_{\perp} = 2.04$, and $A_{\parallel} = 156$ G. FTIR (KBr): 1597 (s), 1576, 1485 (s, C=N_{py}, C=C_{aromatic}), 1456, 1438, 1394, 1276, 1257, 1199, 1098 (s, ClO₄⁻), 1068, 997, 874, 758, 621, 603, 480, 415 cm⁻¹. ESI-MS pos. in MeOH: $m/z = 439$ [[Cu(L^{amine})] + H]⁺. Solution magnetic moment (Evans method, 19.8 °C, 7.0 × 10⁻³ M, acetonitrile-*d*₃): 1.101 μ_B /Cu. Solid state magnetic moment (MSB-Auto, 4.5 kG, 22.0 °C): 1.076 μ_B /Cu.

[Cu₄(L^{amide})₂(H₂O)₅] (**3**). To a 5 mL acetonitrile solution of H₂L^{amide} (0.0600 g, 0.150 mmol) and Et₃N (0.080 mL, 0.60 mmol) was added dropwise a 1 mL acetonitrile solution of Cu(ClO₄)₂·6H₂O (0.0550 g, 0.150 mmol) with constant stirring. The green precipitate was collected by filtration, washed with acetonitrile and diethylether, and dried under vacuum (0.060 g, 70% yield). Anal. Calcd for C₄₆H₄₈Cu₄N₆O₁₃: C, 48.9; H, 4.1; N, 7.4. Found: C, 48.3; H, 4.4; N, 7.4. UV/vis (DMSO) [λ_{max} , nm (ϵ , M⁻¹ cm⁻¹): 306 (23,300), 420 (1310), 640 (310 sh)]. EPR (9.436 GHz, mod. amp. 5.0 G, CH₂Cl₂, 77K): $g_{\parallel} = 2.25$, $g_{\perp} = 2.07$, and $A_{\parallel} = 180$ G. FTIR (KBr): 3368, 3062, 1608 (s, C=O_{amide}), 1576, 1539 (s), 1472 (s, C=N_{py}, C=C_{aromatic}), 1445, 1388, 1328, 1243, 1148, 1121, 757 cm⁻¹. ESI-MS pos. in MeOH/DMSO: $m/z = 467$ [Cu(H₂L^{amide}) + H]⁺ and 489 [Cu(H₂L^{amide}) + Na]⁺. Compound **3** upon recrystallization by slow evaporation of a DMSO/methanol solvent mixture produced dark green crystals of [Cu₆(HL^{amide})₄(H₂O)₂] (**4**). Solution magnetic moment (Evans method, 19.8 °C, 8.0 × 10⁻³ M, DMSO-*d*₆): 1.780 μ_B /Cu. Solid state magnetic moment (MSB-Auto, 4.5 kG, 22.0 °C): 1.765 μ_B /Cu.

X-ray Crystal Structure Determination. Crystal data are summarized in Table 1 and selected bond lengths and angles for **1**, **2**, and **4** are summarized in Table 2. X-ray quality crystals of **1** were obtained by slow evaporation of a methanol solution of **1**. Single crystals of **2** were obtained by diethyl ether diffusion into an acetonitrile solution of **2**. Recrystallization of **3** by slow evaporation of a concentrated DMSO/methanol solution yielded dark green crystals of **4**. Intensity data for all the compounds were

Table 2. Selected Bond Lengths (Å) and Angles (deg) for Complexes **1**, **2**, and **4**

1			
Cu1–N9	2.0020(14)	Cu1–O1	1.9415(12)
Cu1–N20	2.0032(14)	Cu1–O28	1.9370(12)
N9–C8	1.291(2)	Cu1–O29	2.3404(13)
N20–C21	1.287(2)	O28–Cu1–O1	80.81(5)
O1–Cu1–N9	91.21(5)	O28–Cu1–N9	171.11(5)
O1–Cu1–N20	166.68(5)	O28–Cu1–N20	90.71(5)
N9–Cu1–N20	96.40(6)		
2			
Cu1–O1	1.930(3)	Cu2–N9	1.996(4)
Cu1–O28	1.929(3)	Cu2–N20	2.015(4)
Cu2–O1	1.960(3)	Cu2–N1S	2.403(8)
Cu2–O28	1.967(3)	Cu2A–N1SA	2.76(2)
O1–Cu1–O1B	180.0	O28–Cu1–O1	79.14(13)
O1–Cu2–N9	92.91(14)	O28–Cu1–O1B	100.86(13)
O1–Cu2–N20	170.31(16)	O28–Cu1–O28A	179.998(1)
O1–Cu2–O28	77.52(12)	O28–Cu2–N9	170.34(15)
		O28–Cu2–N20	92.88(16)
4			
Cu1A–O1	2.269(7)	Cu2A–O30A	1.905(7)
Cu1A–O1A	1.923(9)	Cu2A–O30C	1.905(7)
Cu1A–O1B	2.122(7)	Cu2A–O23A	1.930(7)
Cu1A–N10A	1.923(10)	Cu2A–O23C	1.930(7)
Cu1A–N14A	1.998(12)	Cu1A–Cu1B	2.892(3)
O1A–Cu1A–O1	79.3(3)	N14A–Cu1A–O1	93.9(3)
O1B–Cu1A–O1	73.6(3)	N14A–Cu1A–O1B	97.6(4)
O1A–Cu1A–O1B	79.3(3)	O30A–Cu2A–O23C	87.1(3)
O1A–Cu1A–N10A	92.2(5)	O30C–Cu2A–O23C	92.6(3)
O1A–Cu1A–N14A	173.1(4)	O30C–Cu2A–O30A	176.2(5)
O23C–Cu2A–O23A	171.2(5)		

collected using a diffractometer with a Bruker APEX ccd area detector¹⁰ and graphite-monochromated Mo K α radiation ($\lambda = 0.71073$ Å). The samples were cooled to 100(2) K. Cell parameters were determined from a nonlinear least-squares fit of the data. The data were corrected for absorption by the semiempirical method.¹¹ The structures were solved by direct methods and refined by full-matrix least-squares methods on F^2 .¹² Hydrogen atom positions of hydrogens bonded to carbons were initially determined by geometry and refined by a riding model. Hydrogens bonded to nitrogens were located on a difference map, and their positions were refined independently. Non-hydrogen atoms were refined with anisotropic displacement parameters. Hydrogen atom displacement parameters were set to 1.2 (1.5 for methyl) times the displacement parameters of the bonded atoms.

The separate solvent molecule in **1** was disordered and was modeled in two orientations. The occupancies of the disordered solvent refined to 0.510(8) and 0.490(8) for the unprimed and primed atoms. Restraints on the positional and displacement parameters of the disordered atoms were required.

Complex **2** was found to sit on a crystallographic center of symmetry. The sample was twinned by a 2-fold rotation about the (1 0 1) direction with a twin ratio refined to 0.301(2). Both sites of acetonitrile were disordered and were modeled in two orientations. The occupancies of the S solvent site refined to 0.698(10) and 0.302(10) for the unprimed and primed atoms. The T solvent site was located near a center of symmetry, and the occupancies refined

(10) (a) *SMART Software Reference Manual*; Bruker-AXS: Madison, WI, 1998. (b) *SAINTE Software Reference Manual*; Bruker-AXS: Madison, WI, 1998.

(11) Sheldrick, G. M. *SADABS. Program for empirical absorption correction of area detector data*; University of Göttingen, Göttingen, Germany, 2002.

(12) (a) Sheldrick, G. M. *SHELXTL Version 6.10 Reference Manual*; Bruker AXS Inc.: Madison, WI, 2000. (b) *International Tables for Crystallography*; Kluwer: Boston, 1995; Vol. C.

to 0.266(3) and 0.234(3) for the unprimed and primed atoms. Restraints on the positional and displacement parameters of the solvent atoms were required.

The intensity data for complex **4** were truncated to 1.09 Å resolution because data in higher resolution shells had $R(\text{int}) > 0.25$. The main molecule was found to sit on a crystallographic 2-fold rotation axis. The oxygen and sulfur atoms of one dimethylsulfoxide, DMSO, molecule break this 2-fold symmetry and thus were given occupancies of 0.5. A separate DMSO molecule was so disordered that it was best modeled using the Squeeze program.¹³ The O3S and O4S sites were disordered and were modeled in two orientations. The occupancies of these atoms were set to (O3S): 0.640(16) and 0.360(16) and (O4S): 0.49(2) and 0.51(2) for the unprimed and primed atoms. Restraints on the positional parameters of the atoms of the bound DMSO and the displacement parameters of two aromatic rings (showing libration) were required.

Results and Discussion

All three ligands were synthesized using 2-methyl-2-pyridin-2-yl-propane-1,3-diamine (ppda) as the precursor.⁸ The diimine ligand $\text{H}_2\text{L}^{\text{imine}}$ was synthesized via a Schiff base condensation of ppda with salicylaldehyde, whereas the diamine ligand $\text{H}_2\text{L}^{\text{amine}}$ was prepared by reducing the diimine formed in situ to the diamine with sodium borohydride. The diamide ligand $\text{H}_4\text{L}^{\text{amide}}$ was synthesized by standard coupling reaction of ppda with salicylic acid. The differences between these three ligands center on coordinating atoms and ligand rigidity: $\text{H}_2\text{L}^{\text{imine}}$ contains rigid C=N double bonds and a potential N_3O_2 donor set, $\text{H}_2\text{L}^{\text{amine}}$ contains more flexible C–N single bonds also with a potential N_3O_2 donor set, and $\text{H}_4\text{L}^{\text{amide}}$ has rigid amide moieties with a potential N_3O_4 donor set. $\text{H}_2\text{L}^{\text{imine}}$ and $\text{H}_2\text{L}^{\text{amine}}$ both contain two ionizable phenol groups, making them -2 anionic ligands when deprotonated, whereas $\text{H}_4\text{L}^{\text{amide}}$ has two phenol groups plus two amide groups, making it a potentially -4 anionic ligand.

The copper complexes of all three ligands were synthesized in the same manner by treating the ligand with triethylamine to deprotonate the ionizable groups (see Scheme 1), followed by addition of copper(II) and isolation through precipitation and/or crystallization. Significant structural variation was observed, both in the nuclearity of the complexes formed and in the coordination modes of the ligands, forming mononuclear $[\text{Cu}(\text{L}^{\text{imine}})(\text{CH}_3\text{OH})]$ (**1**), trinuclear $[\text{Cu}_3(\text{L}^{\text{amine}})_2(\text{CH}_3\text{CN})_2](\text{ClO}_4)_2$ (**2**), or polynuclear complexes $[\text{Cu}_4(\text{L}^{\text{amide}})_2(\text{H}_2\text{O})_4]$ (**3**) and $[\text{Cu}_6(\text{HL}^{\text{amide}})_4(\text{H}_2\text{O})_2]$ (**4**) with each respective ligand.

The X-ray crystal structure of **1** revealed that it contains five coordinate copper(II) ions with square pyramidal geometry, having a τ_5 parameter¹⁴ of 0.074 (Figure 1). A solvent methanol occupies the apical position, and the N_2O_2 ligand donor set from $(\text{L}^{\text{imine}})^{2-}$ occupies the basal plane of the pyramid. The pyridyl N atom of $(\text{L}^{\text{imine}})^{2-}$ does not coordinate to the metal center in **1**, a phenomenon that was observed previously in our laboratory with related guanidiny

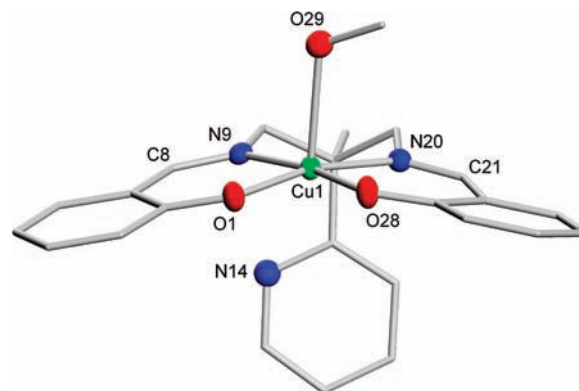


Figure 1. Representation of the X-ray structure of **1** with H atoms removed for clarity.

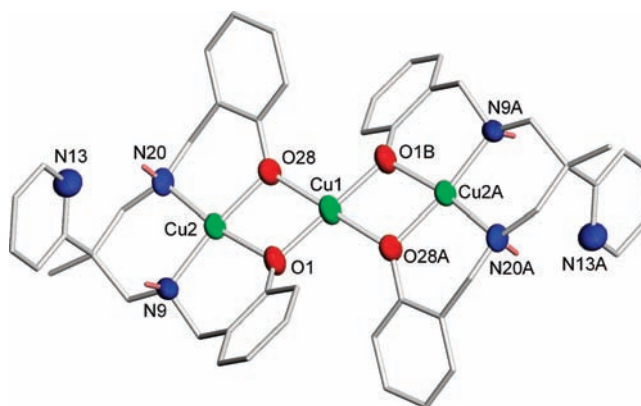


Figure 2. Representation of the X-ray structure of the cationic portion of **2** with CH_3CN ligands and all H atoms except for amine protons removed for clarity.

ligands.¹⁵ The short carbon–nitrogen bond distances in **1** (1.287–1.291 Å) corroborate the imine nature of the ligand.

The X-ray structure of **2** consists of three Cu^{2+} ions arranged in a linear array with two tetradentate $(\text{L}^{\text{amine}})^{2-}$ ligands capping each end (Figure 2). Like in **1**, the pyridyl N atoms of the $(\text{L}^{\text{amine}})^{2-}$ ligands do not coordinate to the copper ions, but in contrast to **1**, the phenolato oxygens bridge to connect two monomer units similar to **1** together via the third copper, Cu1. The overall +2 charge of the complex is balanced by two perchlorate counterions. The two terminal copper ions, Cu2 and Cu2A, are pentacoordinate with square pyramidal geometry ($\tau_5 = 0.0005$) composed of N_2O_2 donor atoms in the basal plane, and a nitrogen atom of a coordinated acetonitrile ligand (not shown) in the apical position. The third copper(II) ion (Cu1), lying at the inversion center of centrosymmetric **2**, links the monomers together via four μ_2 -phenolato oxygen atoms of the two ligands in a square planar environment, with a τ_4 parameter² of zero. The perchlorate counterions interact weakly with Cu1 via the axial positions ($\text{Cu}\cdots\text{O} = 2.594\text{--}2.800$ Å), and through hydrogen bonding with the amine NH groups on $(\text{L}^{\text{amine}})^{2-}$. A prominent peak in the ESI-MS of **2** at $m/z = 439$ corresponds to $\{[\text{Cu}(\text{L}^{\text{amine}})] + \text{H}\}^+$, suggesting that some of **2** dissociates into monomeric species in solution. The solution and solid

(13) van der Sluis, P.; Spek, A. L. *Acta Crystallogr. A* **1990**, *A46*, 194–201.

(14) Addison, A. W.; Rao, T. N.; Reedijk, J.; van Rijn, J.; Verschoor, G. C. *J. Chem. Soc., Dalton Trans.* **1984**, 1349–1356.

(15) Pal Chaudhuri, U.; Powell, D. R.; Houser, R. P. *Inorg. Chim. Acta* [Online early access]. DOI: 10.1016/j.ica.2008.10.030. Published Online: **2008**.

state magnetic moments for **2** of $1.101 \mu_{\text{B}}/\text{Cu}$ and $1.076 \mu_{\text{B}}/\text{Cu}$, respectively, are less than the spin-only value of $1.73 \mu_{\text{B}}/\text{Cu}$, suggesting some antiferromagnetic coupling. The presence of the dimeric species, $[\text{Cu}_2(\text{L}^{\text{amine}})]^{2+}$, was not observed in the ESI-MS, but the solution magnetic data suggests that it is, in fact, present. The typical axial EPR spectrum of **2** indicates the presence of some unpaired spin, consistent with the notion that **2** dissociates in solution into paramagnetic $[\text{Cu}(\text{L}^{\text{amine}})]$ and diamagnetic $[\text{Cu}_2(\text{L}^{\text{amine}})]^{2+}$. The UV/vis spectra of **2** at different concentrations were compared to assess the dissociation of trimeric **2** into monomers and dimers, but no changes were observed, suggesting that even at high concentration **2** dissociates into $[\text{Cu}(\text{L}^{\text{amine}})]$ and $[\text{Cu}_2(\text{L}^{\text{amine}})]^{2+}$.

Complex **3**, which based on analytical data can be formulated as either $[\text{Cu}_4(\text{L}^{\text{amide}})_2(\text{H}_2\text{O})_4]$ or $[\text{Cu}_2(\text{L}^{\text{amide}})(\text{H}_2\text{O})_2]$, was isolated as a green precipitate. Recrystallization from a methanol/DMSO solution yielded dark green crystals of $[\text{Cu}_6(\text{HL}^{\text{amide}})_4(\text{H}_2\text{O})_2]$ (**4**), where $(\text{HL}^{\text{amide}})^{3-}$ is the triply deprotonated form of $\text{H}_4\text{L}^{\text{amide}}$. The ESI-MS of **3** dissolved in DMSO/MeOH displayed prominent peaks at $m/z = 467$ and 489 corresponding to monomeric $\{[\text{Cu}(\text{H}_2\text{L}^{\text{amide}}) + \text{H}]^+\}$ and $\{[\text{Cu}(\text{H}_2\text{L}^{\text{amide}}) + \text{Na}]^+\}$, respectively. The observation of a doubly deprotonated ligand in the ESI-MS of **3** and a triply deprotonated ligand in the crystal structure of **4** suggests that the protonation and deprotonation of the amidic protons is in equilibrium in solution. The observation of these peaks in the ESI-MS also reveals that, similar to **2**, at least some of **3** dissociates into monomeric species in solution. To further probe this question, UV/vis spectra of **3** taken at variable concentrations were compared. However, no changes in the peak positions in the UV/vis spectra of **3** at different concentrations were observed. Complex **3** possesses an axial EPR spectrum, and the solution and solid-state magnetic moments for **3** are $1.780 \mu_{\text{B}}/\text{Cu}$ and $1.765 \mu_{\text{B}}/\text{Cu}$, respectively, indicating the absence of any magnetic coupling either in solution or in the solid state. Taken together, the data suggest that **3** very likely dissociates into smaller, perhaps monomeric, species in solution.

The crystal structure of **4** (Figure 3) consists of six copper(II) ions, four triply deprotonated $(\text{HL}^{\text{amide}})^{3-}$ ligands, and two water ligands. The highly symmetrical structure has two different copper coordination environments. The ligands in **4** are color-coded in Figure 3 to illustrate the way each symmetrically equivalent ligand coordinates to three copper ions. Both ends of the structure are capped by bis(μ -phenoxo) μ - H_2O -dicopper units. The bridging phenoxo groups are provided by two separate ligands, which also coordinate to Cu1A and Cu1B via amidate and pyridyl groups. Water ligands bridge the two copper centers (Cu1A and Cu1B), making these copper ions pentacoordinate with geometries intermediate between the idealized square-pyramidal and trigonal-bipyramidal ($\tau_5 = 0.466$). This type of coordination geometry has been described as trigonally distorted rectangular pyramidal.¹⁴ The copper–copper distance between Cu1A and Cu1B is $\sim 2.89 \text{ \AA}$. The second amide/phenolate arm of each ligand coordinates to the other copper ions, Cu2A and Cu2B, via the amide O and phenolate O atoms in

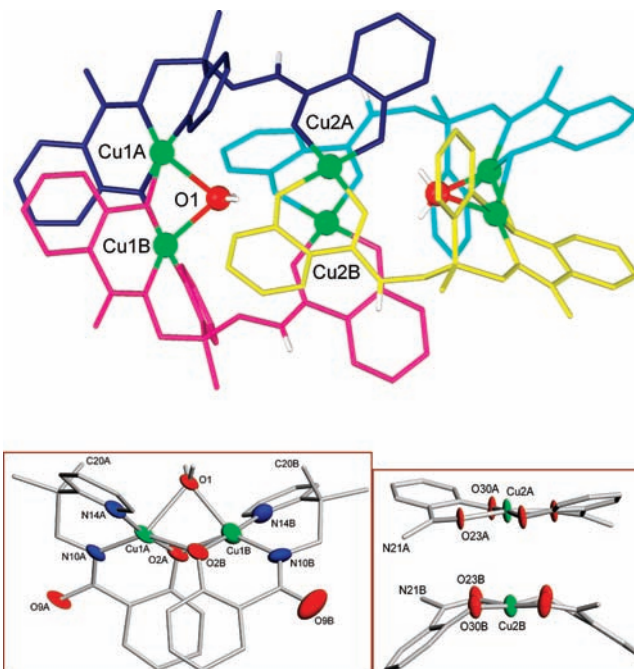


Figure 3. Representation of the X-ray crystal structure of **4** (top). Isolated coordination environments for Cu1A and Cu1B (bottom left) and Cu2A and Cu2B (bottom right). All H atoms except for amide and water H atoms omitted for clarity.

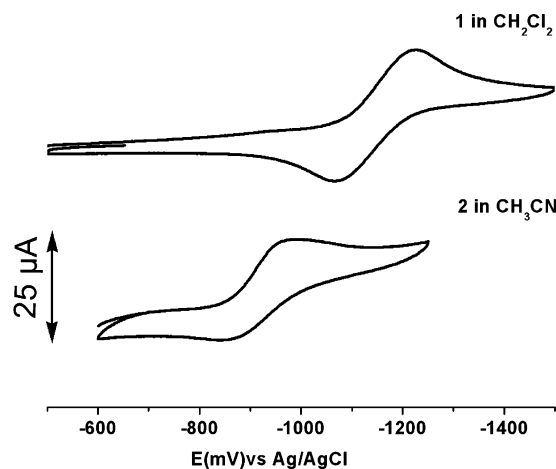


Figure 4. CVs (scan rate = 100 mV s^{-1} ; 0.1 M TBAH supporting electrolyte) of a 1.0 mM solution of **1** in CH_2Cl_2 (top) and a 1.0 mM solution of **2** in CH_3CN (bottom).

a distorted square planar geometry ($\tau_4 = 0.09$). The distance between Cu2A and Cu2B, which are stacked but staggered by $\sim 45^\circ$, is 3.49 \AA . Intramolecular hydrogen bonding between the coordinated water ligands and the phenolate oxygens in the middle of the structure ($\text{O1-H}\cdots\text{O23}$ and $\text{O1-H}\cdots\text{O30}$), as well as intermolecular hydrogen bonding between the amide NH groups from one molecule and amide O groups from adjacent molecules ($\text{N21-H}\cdots\text{O9}$) add stability to the structure of **4**.

The redox properties of **1–3** were studied by cyclic voltammetry in dichloromethane (**1**), acetonitrile (**2**), or DMSO (**3**). The cyclic voltammograms (CVs) of **1** and **2** showed reversible processes with $E_{1/2} = -1125 \text{ mV}$ versus Ag/AgCl and $\Delta E = 137 \text{ mV}$ for **1**, and $E_{1/2} = -914 \text{ mV}$ versus Ag/AgCl and $\Delta E = 139 \text{ mV}$ for **2** (Figure 4). These

are attributed to the Cu(II)/Cu(I) redox couple. For **2**, an irreversible peak was also observed at $E_{pc} = -152$ mV, and during the reverse scan a spike was observed at -166 mV which was likely due to the deposition of metallic copper at the electrode surface by decomposition of the compound.¹⁶ The CV of complex **3** contained only irreversible redox features. None of the complexes displayed any of the ligand-centered processes typically seen for copper complexes with *tert*-butyl substituted salen ligands.⁷

In summary, three new pyridylbis(phenol) ligands with diimine, diamine, or diamide linkages were designed and synthesized. Copper(II) complexes of varying nuclearity were synthesized with these ligands. Interestingly, the ligands in

(16) Koval, I. A.; Huisman, M.; Stassen, A. F.; Gamez, P.; Lutz, M.; Spek, A. L.; Reedijk, J. *Eur. J. Inorg. Chem.* **2004**, 591–600.

1 and **2** coordinate via the imine/amine nitrogens and phenolato oxygens, but not through the pyridyl groups, while the ligands in **4** do coordinate via the pyridyl group, producing a larger, more complex cluster.

Acknowledgment. This work was supported by the National Science Foundation (NSF CHE-0616941). Additionally, we thank the NSF for the purchase of a CCD-equipped X-ray diffractometer (CHE-0130835).

Supporting Information Available: Crystallographic data in CIF file format. This material is available free of charge via the Internet at <http://pubs.acs.org>.

IC9000768